Electronic Supplementary Information:

Modelling viscoelastic relaxation mechanisms in thermorheologically complex Fe(III)-poly(acrylic acid) hydrogels

Arthur Lenoch[a,b], Monika Schönhoff[a,b], Cornelia Cramer[a,b]

[a] *Center for Soft Nanoscience, Busso-Peus-Str.10, 48149 Münster, Germany.*
[b] *Institut für Physikalische Chemie, University of Muenster, Corrensstraße 28/30, 48149 Münster, Germany.*
E-mail: *cramerc@uni-muenster.de*

ESI1 Real and imaginary parts of complex moduli

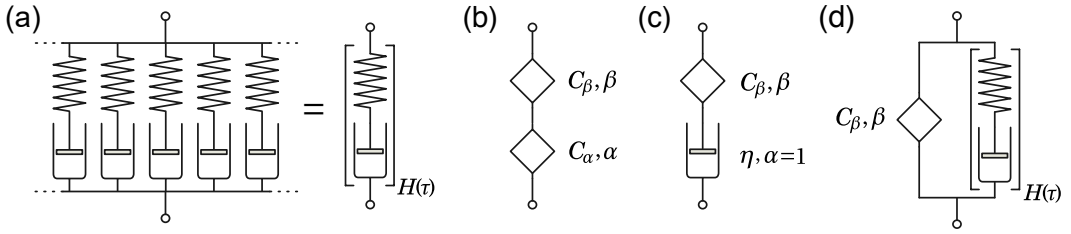

(a) Generalized Maxwell Model (GMM)

$$\widehat{G}(\omega) = G' + iG'' = \int_{-\infty}^{\infty} H(\tau)\frac{i\omega\tau}{1+i\omega\tau}\,\mathrm{d}\ln\tau$$

$$G'(\omega) = \int_{-\infty}^{\infty} H(\tau)\frac{(\omega\tau)^2}{1+(\omega\tau)^2}\,\mathrm{d}\ln\tau$$

$$G''(\omega) = \int_{-\infty}^{\infty} H(\tau)\frac{\omega\tau}{1+(\omega\tau)^2}\,\mathrm{d}\ln\tau$$

(c) Fractional Maxwell Liquid (FML)

$$\widehat{G}(\omega) = G' + iG'' = \frac{\eta C_\beta (i\omega)^\beta}{\eta + C_\beta (i\omega)^{\beta-1}}$$

$$G'(\omega) = \frac{\eta^2 C_\beta \omega^{2+\beta}\cos\left(\frac{\pi}{2}\beta\right)}{(\eta\omega)^2 + \left(C_\beta\omega^\beta\right)^2 + 2\eta C_\beta\omega^{1+\beta}\cos\left(\frac{\pi}{2}(1-\beta)\right)}$$

$$G''(\omega) = \frac{\eta C_\beta \omega^{1+\beta}\left[C_\beta\omega^\beta + \eta\omega\sin\left(\frac{\pi}{2}\beta\right)\right]}{(\eta\omega)^2 + \left(C_\beta\omega^\beta\right)^2 + 2\eta C_\beta\omega^{1+\beta}\cos\left(\frac{\pi}{2}(1-\beta)\right)}$$

(b) Fractional Maxwell Model (FMM)

$$\widehat{G}(\omega) = G' + iG'' = \frac{C_\alpha (i\omega)^\alpha \cdot C_\beta (i\omega)^\beta}{C_\alpha (i\omega)^\alpha + C_\beta (i\omega)^\beta}$$

$$G'(\omega) = \frac{C_\alpha\omega^\alpha C_\beta\omega^\beta\left[C_\beta\omega^\beta\cos\left(\frac{\pi}{2}\alpha\right) + C_\alpha\omega^\alpha\cos\left(\frac{\pi}{2}\beta\right)\right]}{(C_\alpha\omega^\alpha)^2 + \left(C_\beta\omega^\beta\right)^2 + 2C_\alpha\omega^\alpha C_\beta\omega^\beta\cos\left(\frac{\pi}{2}(\alpha-\beta)\right)}$$

$$G''(\omega) = \frac{C_\alpha\omega^\alpha C_\beta\omega^\beta\left[C_\beta\omega^\beta\sin\left(\frac{\pi}{2}\alpha\right) + C_\alpha\omega^\alpha\sin\left(\frac{\pi}{2}\beta\right)\right]}{(C_\alpha\omega^\alpha)^2 + \left(C_\beta\omega^\beta\right)^2 + 2C_\alpha\omega^\alpha C_\beta\omega^\beta\cos\left(\frac{\pi}{2}(\alpha-\beta)\right)}$$

(d) Generalized Maxwell Model + Fractional Springpot

$$\widehat{G}(\omega) = G' + iG'' = \int_{-\infty}^{\infty} H(\tau)\frac{i\omega\tau}{1+i\omega\tau}\,\mathrm{d}\ln\tau + C_\beta (i\omega)^\beta$$

$$G'(\omega) = \int_{-\infty}^{\infty} H(\tau)\frac{(\omega\tau)^2}{1+(\omega\tau)^2}\,\mathrm{d}\ln\tau + C_\beta\omega^\beta\cos\left(\frac{2\pi}{2}\right)$$

$$G''(\omega) = \int_{-\infty}^{\infty} H(\tau)\frac{\omega\tau}{1+(\omega\tau)^2}\,\mathrm{d}\ln\tau + C_\beta\omega^\beta\sin\left(\frac{2\pi}{2}\right)$$

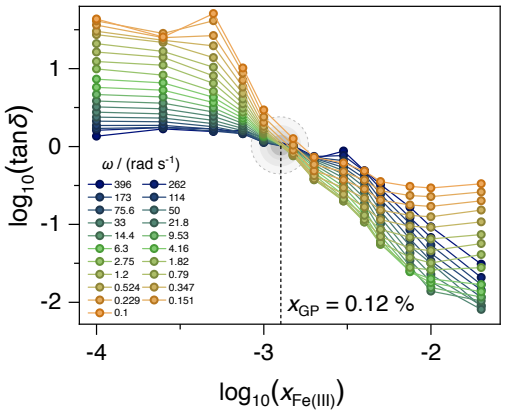

Figure S1. Application of the Winter-Chambon criterion for Fe-PAA hydrogels: at the gel point ($x_{\mathrm{Fe(III)}} = n_{\mathrm{Fe(III)}}/n_{\mathrm{PAA}} = 0.12\,\%$) the loss factor $\tan\delta = G''/G'$ becomes frequency independent, resulting in a crossover when $\tan\delta$ is plotted against the crosslinker fraction. [1]

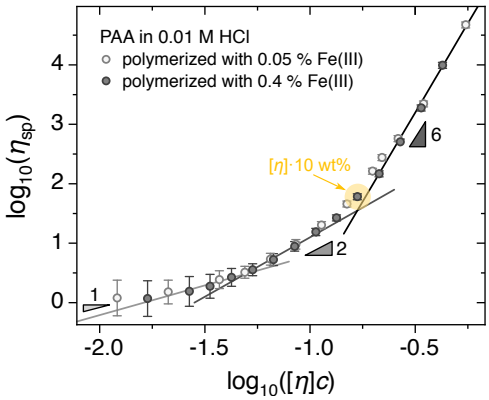

Figure S2. Specific viscosity $\eta_{\mathrm{sp}} = (\eta_0 - \eta_{\mathrm{solvent}})/\eta_{\mathrm{solvent}}$ of pure PAA solutions as a function of the quantity $c[\eta]$, for two molar fractions (relative to monomer) of ferric ions present during polymerization. c was varied from 1 wt% to 30 wt%. Intrinsic viscosities $[\eta]$ were determined by using the Martin equation $\log_{10}(\eta_{\mathrm{sp}}/c) = \log_{10}[\eta] + K[\eta]c$. [2] The weight fraction 10 % used in the hydrogel samples is indicated.

ESI2 Molar mass estimation of PAA

Experimental: Molar masses of the PAA gels were estimated via a diffusion coefficient measurement. A calibration with commercially available PAA of different molar masses (Sigma-Aldrich: 2000 g/mol, 5100 g/mol, 15 000 g/mol, 250 000 g/mol; Polysciences: 50 000 g/mol) was conducted for this purpose. All Fe(III) from two samples with 0.05 % and 0.4 % was removed by dialysis as explained in the main text. Dilute PAA solutions with 0.5 wt% polymer were prepared with acidic 0.1 M DCl solution in D_2O in order to ensure full protonation. PFG-NMR measurements were measured on a 400 MHz NMR spectrometer (AVANCE III HD 400, Bruker BioSpin, Ettlingen, Germany), equipped with a gradient probe head (DIFFBB, Bruker BioSpin). Signal attenuation of the PAA signal was obtained in a stimulated echo pulse sequence, where the maximum gradient strength G was varied from 2 T/m to 4 T/m, while the gradient pulse duration and diffusion time were chosen as δ = 1 ms and Δ = 100 ms, respectively.

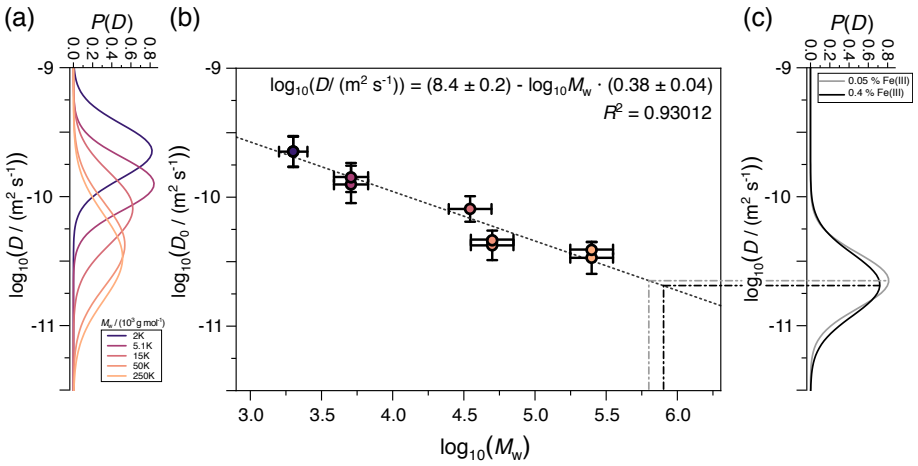

Figure S3. Estimation of the PAA molar mass by means of a diffusion NMR spectroscopy calibration. (a) Diffusion coefficient distributions for commercial PAA samples with M_{w}, as reported by the manufacturer. (b) Calibration curve of the principal diffusion coefficient D_0. (c) Diffusion coefficient distributions of two PAA samples with different ferric ion fractions present during polymerization.

Analysis: The concept of a pulsed field gradient-NMR experiment is described in [3]. As reported in literature [4, 5], the signal attenuation curves of polymers in dilute solution can be modelled by a assuming a probability distribution $P(D)$ of diffusion coefficients:

$$\frac{I}{I_0} = \int_{-\infty}^{\infty} P(D) \exp\left[-\left(\gamma^2 G^2 \delta^2 (\Delta - \delta/3)\right) \cdot D\right] \mathrm{d}\ln D, \tag{1}$$

where γ is the gyromagnetic ratio of the ^{1}H nucleus. Commonly, a log-normal distribution is assumed for $P(D)$:

$$P(D) = \frac{1}{\sqrt{2\pi}\sigma} \exp\left[-\frac{(\ln D - \ln D_0)^2}{2\sigma^2}\right]. \tag{2}$$

Fig. S3(a,b) shows the probability distributions and a calibration curve relating the principal diffusion coefficient of several commercial PAA samples to M_w, as reported by the manufacturer. Fig. S3(c) shows $P(D)$ for two PAA-samples where ferric ions were removed by dialysis, leading to an estimate of $M_{\mathrm{w},0.05} = (7 \pm 2) \cdot 10^5$ g mol^{-1} and $M_{\mathrm{w},0.4} = (6 \pm 2) \cdot 10^5$ g mol^{-1}.

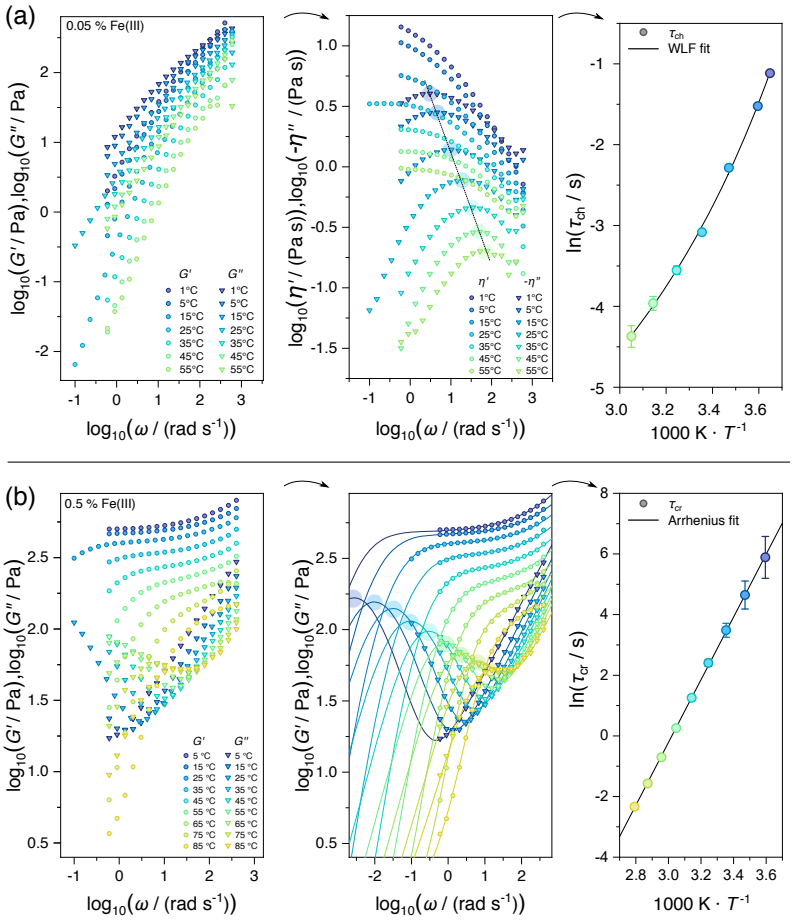

Figure S4. Examples for the determination of temperature-dependent relaxation times: **(a)** τ_{ch} for a sample below the gel point ($x_{\mathrm{Fe(III)}} = 0.05\,\%$). The complex shear modulus is converted to the complex viscosity by $\hat{\eta} = \hat{G}/(i\omega)$, where the imaginary part $-\eta''$ shows a maximum at $\omega = \tau_{\mathrm{ch}}^{-1}$. The relaxation times, displayed as filled circles, are then fitted with the Williams-Landel-Ferry equation (10). **(b)** τ_{cr} for a sample above the gel point ($x_{\mathrm{Fe(III)}} = 0.5\,\%$). Here, G'' shows a maximum at $\omega = \tau_{\mathrm{cr}}^{-1}$, which can be extrapolated by the use of the model discussed in the main text if no apparent maximum is visible. The relaxation times τ_{cr} are fitted to an Arrhenius model.

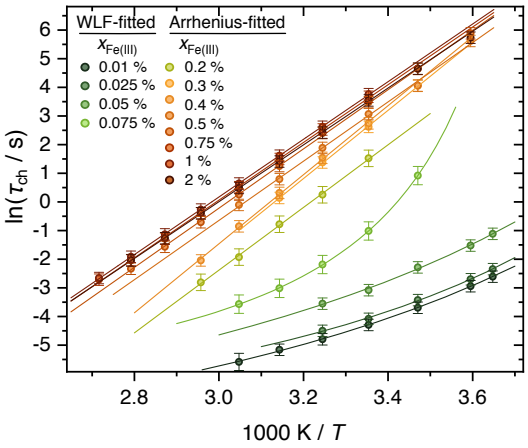

Figure S5. Arrhenius plot of all relaxation times determined directly from raw data for samples below the gel point (τ_{ch}, from maximum of $-\eta''$) and above the gel point (τ_{cr}, from maximum of G''), respectively.

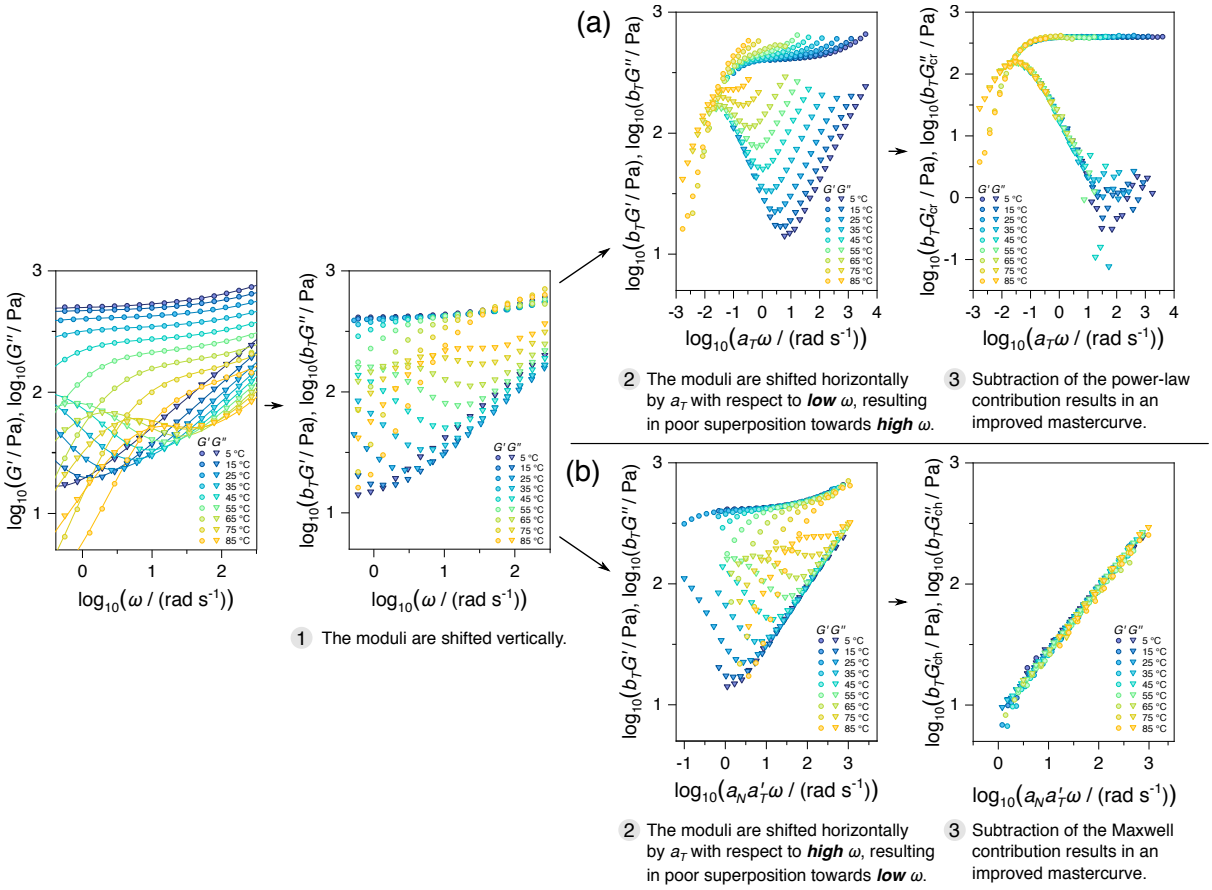

Figure S6. Example for time temperature superposition of separate relaxation modes ($x_{\mathrm{Fe(III)}} = 0.5\,\%$). After vertical shifting, horizontal shifting towards **(a)** low ω or **(b)** high ω fails to superimpose the dynamic moduli adequately across the entire ω-range. Subtracting of either the high-frequency or low-frequency contribution, respectively, improves the superposition quality.

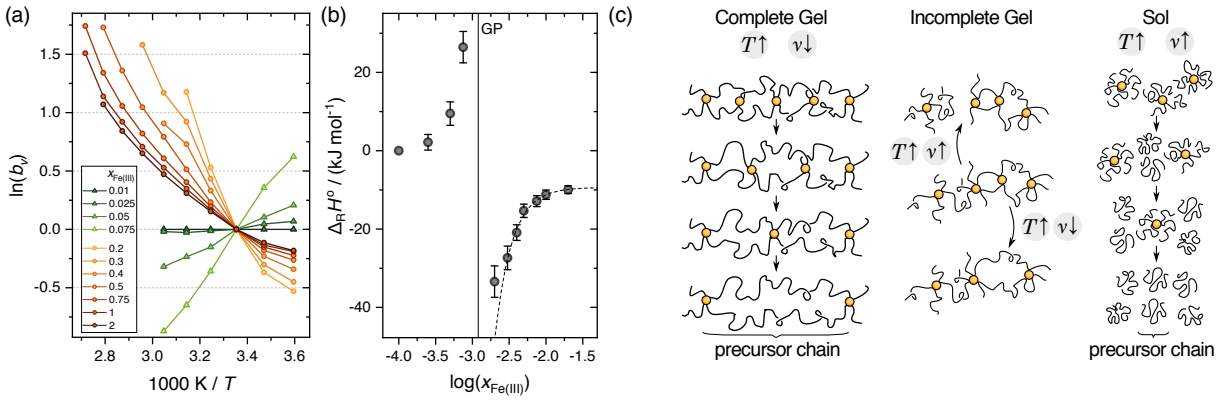

Figure S7. (a) Vertical shift factors b_ν obtained from experimental shift factors b_T by $b_T = b_\nu T_{\mathrm{ref}}/T$. **(b)** Enthalpy values obtained from the local slope at 25 °C from the relation $\ln(b_\nu) = \ln\left(\nu(T_{\mathrm{ref}})/\nu(T)\right) = \left(\Delta_{\mathrm{R}}H^\circ/R\right)\cdot\left(T^{-1} - T_{\mathrm{ref}}^{-1}\right)$. As this approximation is valid for networks far above the gel point, data are extrapolated with an exponential fit to obtain $\Delta_{\mathrm{R}}H^\circ = 9.4\,\mathrm{kJ\,mol^{-1}}$ for $x_{\mathrm{Fe(III)}} \to \infty$. **(c)** Sketch explaining the reversal of b_ν: in a complete gel, the number density ν of network chains decreases with increasing T as crosslinks break; in an incomplete gel just above the gel point, crosslink dissociation leads both to an increase or decrease in ν, depending on the connectivity of the crosslink; in the sol, ν of isolated chains increases with increasing T.

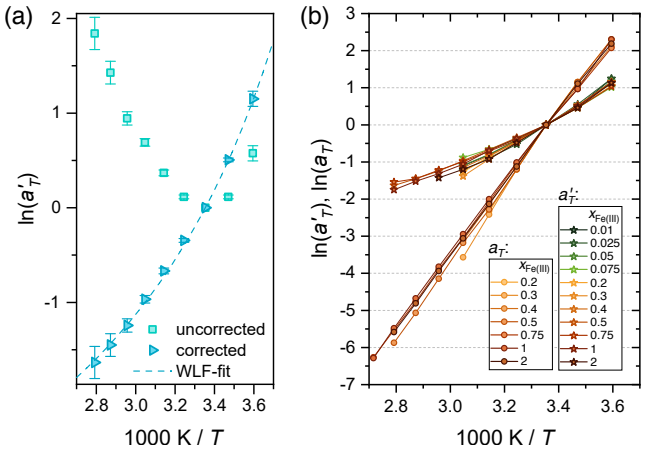

Figure S8. (a) Horizontal shift factors a'_T obtained from high-frequency guided time-temperature superposition, before and after correction by an additional shift factor $a_N = b_\nu^2$. **(b)** Summary of all horizontal shift factors a_T (low-frequency guided TTS) and a'_T (high-frequency guided TTS) for different ferric ion fractions. Lines between points are guide to the eye.

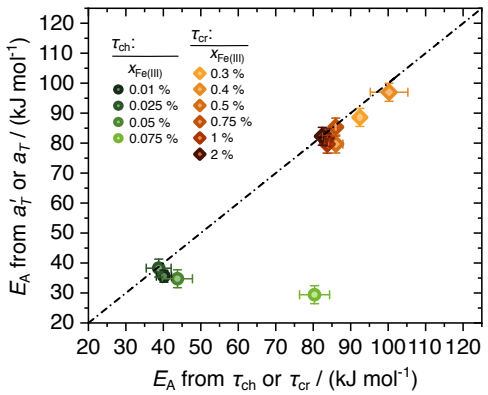

Figure S9. Comparison of activation energies determined by two methods: 1. from T-dependent terminal relaxation times τ_{ch} (Rouse relaxation time of chains), τ_{cr} (relaxation time of crosslink dissociation) and 2. from time temperature superposition. Values for samples below the gel point are represented as circles, for samples above the gel point as diamonds.

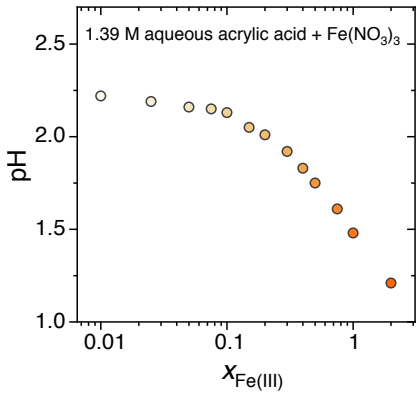

Figure S10. Solution pH of aqueous acrylic acid (10 wt%, corresponding to 1.39 M) with different molar fractions (relative to acrylic acid) of $Fe(NO_3)_3$.

ESI3 Comment on the equivalence of VFT and WLF approaches

The Williams-Landel-Ferry formalism is a common method to model the temperature dependence of the reduced relaxation time in viscoelastic polymer materials: [6]

$$\log_{10}\left(\frac{\tau(T)}{\tau(T_{\mathrm{ref}})}\right) = \frac{-C_1(T-T_{\mathrm{ref}})}{C_2+(T-T_{\mathrm{ref}})}, \tag{3}$$

where C_1, C_2 are fit parameters. This expression is equivalent to the Vogel-Fulcher-Tammann (VFT) equation, which is common in literature discussing dielectric relaxation [7, 8] or the viscosity of glass-forming liquids [9]:

$$\tau(T) = \tau_0 \exp\left(\frac{B}{T-T_0}\right), \tag{4}$$

where τ_0 and B are fit parameters and T_0 is the Vogel-temperature. The fit parameters of both models can be related by:

$$C_1 = B/(T_{\mathrm{ref}}-T_0) \tag{5}$$

$$C_2 = (T_{\mathrm{ref}}-T_0) \tag{6}$$

References

(1) H. H. Winter, in *Encyclopedia of Polymer Science and Technology*, Wiley, 2002, vol. 10, pp. 132–144.

(2) W.-M. Kulicke and C. Clasen, *Viscosimetry of polymers and polyelectrolytes*, Springer Science & Business Media, 2004.

(3) Y. Cohen, L. Avram and L. Frish, "Diffusion NMR spectroscopy in supramolecular and combinatorial chemistry: an old parameter—new insights", *Angewandte Chemie International Edition*, 2005, **44**, 520–554.

(4) X. Guo, E. Laryea, M. Wilhelm, B. Luy, H. Nirschl and G. Guthausen, "Diffusion in Polymer Solutions: Molecular Weight Distribution by PFG-NMR and Relation to SEC", *Macromolecular Chemistry and Physics*, 2017, **218**, 1600440.

(5) M. Röding, D. Bernin, J. Jonasson, A. Särkkä, D. Topgaard, M. Rudemo and M. Nydén, "The gamma distribution model for pulsed-field gradient NMR studies of molecular-weight distributions of polymers", *Journal of Magnetic Resonance*, 2012, **222**, 105–111.

(6) J. D. Ferry, *Viscoelastic properties of polymers*, John Wiley & Sons, New York, Third edition, 1980.

(7) M. Tress, K. Xing, S. Ge, P. Cao, T. Saito and A. Sokolov, "What dielectric spectroscopy can tell us about supramolecular networks", *The European Physical Journal E*, 2019, **42**, 1–12.

(8) F Stickel, E. W. Fischer and R. Richert, "Dynamics of glass-forming liquids. I. Temperature-derivative analysis of dielectric relaxation data", *The Journal of Chemical Physics*, 1995, **102**, 6251–6257.

(9) C. A. Angell, C. T. Imrie and M. D. Ingram, "From simple electrolyte solutions through polymer electrolytes to superionic rubbers: some fundamental considerations", *Polymer International*, 1998, **47**, 9–15.